



# Potassium bromide, $\text{KBr}/\varepsilon$ : New Force Field

Raúl Fuentes-Azcatl\*, Marcia C. Barbosa

Instituto de Física, Universidade Federal do Rio Grande do Sul, Caixa Postal 15051, 91501-970, Porto Alegre, RS, Brazil



## ARTICLE INFO

### Article history:

Received 25 July 2017

Available online 29 September 2017

### Keywords:

KBr

Monovalent ions

Dielectric constant

## ABSTRACT

We propose a new force field for the Potassium Bromide, the  $\text{KBr}/\varepsilon$ . The crystal density and structure, as well as, the density, the viscosity and the dielectric constant of the solution in water were computed and compared with the experiments and other atomistic models. Next, the transferability of the  $\text{KBr}/\varepsilon$  and of the  $\text{NaCl}/\varepsilon$  models is verified by creating the  $\text{KCl}/\varepsilon$  and the  $\text{NaBr}/\varepsilon$  models. The strategy was to employ the same parameters obtained for the  $\text{NaCl}/\varepsilon$  and for the  $\text{KBr}/\varepsilon$  force fields for the building up of the  $\text{KCl}/\varepsilon$  and the  $\text{NaBr}/\varepsilon$  models. The thermodynamic and dynamic properties of these two new models were compared with the experimental

© 2017 Elsevier B.V. All rights reserved.

## 1. Introduction

The potassium Bromide salt shows a number of applications in medicine particularly in the metabolic regulation [1]. The potassium levels influence physiological processes, including [1–3] the cellular-membrane potential, the propagation of action potentials in neuronal, in the muscular, and in the cardiac tissue. Recent studies suggest that the bromine is necessary for the tissue development [4–6] and it participates in the antiparasitic enzyme in the human immune system.

The salt interaction with the biological system is quite complex and experiments even though very important are unable to isolate the properties of the individual molecule–molecule interaction. Therefore, one strategy to understand the interaction of the KBr with other molecules is the use of simulations. The crucial step in the simulations is to construct an appropriated force field for the interaction potential between the ions. The usual method it is to fit the parameters of the model with the experimental results for the density and for the structure for the real system at one determined pressure and temperature. Then, the results obtained for the thermodynamic and the dynamic properties with the model are compared with experiments. Following this procedure, atomistic models for KBr have been proposed [7]. Unfortunately, even though capable of reproducing the density of the system at 298 K and 1 bar the traditional models fail in reproducing other properties such as the dielectric constant of the solution in water, the viscosity and the solubility.

Recently new nonpolarizable models for salt solutions have been proposed. They are inspired by the recent need to understand the behavior of salt in surfaces and confined geometries and in the solubility where the dielectric discontinuity plays quite a relevant role [8–10]. Within these new approaches we proposed a new model for Sodium Chloride [11], the  $\text{NaCl}/\varepsilon$ , which combines Lennard-Jones interactions with Coulombic forces to model the ion interactions. This model is able to reproduce not only the density, but the dielectric constant, the viscosity and the solubility of this salt in the aqueous solution, as well as, the density of the pure system at different temperatures. The basic idea behind the model is to correct for the nonpolarizability of the Coulombic term by introducing a screening factor in the ionic charge. The assumption that polarizable system for some temperature and pressures can be reduced to simple nonpolarizable models was introduced by Leontyev and Stuchebrukhov [12]. This strategy was then used by Kann and Skinner [13] by adapting the Mao and Pappu

\* Corresponding author.

E-mail address: [razcatl@xanum.uam.mx](mailto:razcatl@xanum.uam.mx) (R. Fuentes-Azcatl).

**Table 1**  
Force field parameter of KBr/ $\epsilon$ .

Model	q/e	$\lambda_c$	$\sigma/\text{\AA}$	$(\epsilon/k_B)/\text{K}$
K	+1	0.885	2.86	115.83
Br	−1	0.885	4.057	287.47

model [14] to study the mobility of salt in water. The main difference between our NaCl/ $\epsilon$  [11] and the proposition of Kann and Skinner [13] is that the parametrization of the screening was fixed by the dielectric constant of the ion–ion Coulombic potential while in our case the parameters were selected to give the experimental dielectric constant of the water solution at 1 bar and 298 K and the density and the structure of crystal. This was possible because we used improved water models that reproduce various experimental values such as the dielectric constant at various conditions of pressure and temperature [15–17]. Our results for the NaCl were then checked for a wide range of densities showing a very good agreement with the experiments [11].

Here we explore the same method to propose a force field for the KBr. Then, since in principle very similar screening should be expected for the monovalent salt solutions, the same parametrization already obtained for the pure ions in the NaCl and KBr solutions were tested without any additional fitting for the NaBr and KCl salt solutions.

The remaining of the paper goes as follows. In Section 2 the new model, the KBr/ $\epsilon$ , is introduced and the TIP4P/ $\epsilon$  water model was reviewed. Section 3 summarizes the simulation details and simulational results for the KBr/ $\epsilon$ , the KCl/ $\epsilon$  and the NaBr/ $\epsilon$  models are compared with experimental results in Section 4. Conclusions of the robustness of our models are presented in Section 5.

## 2. The models

### 2.1. The KBr/ $\epsilon$ model

The ions of the salt are modeled as spherical particles interacting through the potential

$$u(r_{ij}) = 4\epsilon_{ij} \left[ \left( \frac{\sigma_{ij}}{r_{ij}} \right)^{12} - \left( \frac{\sigma_{ij}}{r_{ij}} \right)^6 \right] + \lambda_i \lambda_j \frac{q_i q_j}{4\pi \epsilon_0 r_{ij}} \quad (1)$$

where  $r_{ij}$  is the distance between ions  $i$  and  $j$ ,  $q_i$  is the electric charge of ion  $i$ ,  $\epsilon_0$  is the permittivity of vacuum,  $\epsilon_{ij}$  is the Lennard-Jones energy that is used as energy scale and  $\sigma_{ij}$  is the distance between the ions, used as length scale.

For the interaction between the ions and the water molecules, the Lorentz–Berteloth rule is employed [18], namely

$$\sigma_{\alpha\beta} = \left( \frac{\sigma_{\alpha\alpha} + \sigma_{\beta\beta}}{2} \right); \quad \epsilon_{\alpha\beta} = \sqrt{\epsilon_{\alpha\alpha} \epsilon_{\beta\beta}}. \quad (2)$$

For the KBr/ $\epsilon$  model the Lennard-Jones (LJ) energy,  $\epsilon_{ij} = \epsilon_{LJ}$ , and the distance scale,  $\sigma_{ij} = \sigma_{LJ}$ , are the same for any  $i$  and  $j$  namely K–K, K–Br or Br–Br. The ion charges are  $q_i = \pm 1 e$  where  $e$  is the charge of an electron.

The original assumption was to include effects due to water polarization by adding to a rigid model a screening term [11–13]. Here we adapt this proposition for the KBr salt model. Then the screening parameter becomes  $\lambda_i = \lambda_c$ . Therefore, our interaction potential of the ions has three parameters, namely  $\lambda_c$ ,  $\sigma_{LJ}$  and  $\epsilon_{LJ}$  to be adjusted with experimental data for each ion. These parameters are selected so the KBr/ $\epsilon$  force field reproduces the experimental value for the density of the crystal in the face centered cubic phase at the 298 K of temperature [7,19] and 1 bar. These procedure allows for a number of possible parameters values. This degeneracy is broken by selecting the subset that also gives the radial distribution function,  $g(r)$ , which gives the appropriate behavior of the salt crystal at 298 K of temperature and 1 bar of pressure.

The next step is this reduction in the parameter space is to select the set of values that also gives the proper density and the dielectric constant in the mixture of the salt with water [19] at 298 K of temperature and 1 bar of pressure. These last step was done using a solution with 4 molal of salt concentration and the TIP4P/ $\epsilon$  water model. The final result for the force field for the KBr/ $\epsilon$  model is shown in Table 1.

### 2.2. TIP4P/ $\epsilon$ water model

The TIP4P/ $\epsilon$  [15] water is illustrated in Fig. 1. The intermolecular force is given by the Lennard Jones and the Coulomb interactions as given by Eq. (2). The positive charges are located at each hydrogen and the negative charge which neutralizes the molecule is placed along the bisector of the HOH angle located at distance  $l_{OM}$  of the oxygen as shown in Fig. 1. The parameters of the Force Fields for the TIP4P/ $\epsilon$  are given in the Table 2 with  $\lambda_O = \lambda_H = 1$  in Eq. (2).

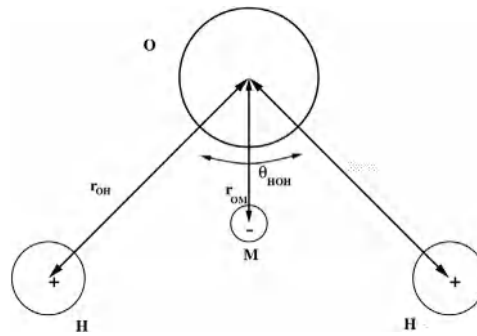


Fig. 1. The TIP4P/ε Model.

**Table 2**Force field parameters of TIP4P/ε water model. The charge in site M is  $q_M = -(2q_H)$ .

Model	$r_{OH}/\text{Å}$	$\Theta/^\circ$	$q_H/e$	$q_M/e$	$r_{OM}/\text{Å}$	$\sigma/\text{Å}$	$(\epsilon/k_B)/\text{K}$
TIP4P/ε	0.9572	104.52	0.527	1.054	0.105	3.165	93

**Table 3**

Composition of KBr solutions used in the simulations at 298.15 K and 1 bar.

Molality (m)	$N_{H_2O}$	$N_{ions}$
0.99	832	32
1.99	806	58
3.07	778	86
4.05	754	110
5.0	732	132

### 3. The simulation details

Molecular dynamic (MD) simulations were performed using GROMACS [20]. The equations of motion were solved using the leap-frog algorithm [20,21] with 2 fs time steps. The total time for the simulation for different molalities is 30 ns, keeping the positions and velocities for every 500 steps.

For the shear viscosity shorter times steps and longer simulations were employed, 1 fs and 40 ns respectively. The Coulombic forces were treated via Ewald summations with the real part of the Coulombic potential truncated at 10 Å. The Fourier component of the Ewald sums was evaluated by using the smooth particle mesh Ewald (SPME) method [22] with a grid spacing of 1.2 Å and a fourth degree polynomial for the interpolation. The simulation box is cubic throughout the whole simulation and the geometry of the water molecules kept constant using the LINCS procedure [23]. The NpT ensemble was employed with the Nosé Hoover thermostat [24] and the Parrinello–Rahman barostat with a  $\tau_p$  parameter of 1.0 ps [20].

The MD simulations for the pure KBr were carried out under 1 bar pressure condition, on a system of 1024 KBr pairs, with a time step  $\Delta t = 2$  fs, the time of simulations is 10 ns and storing the positions and velocities every 1000 simulation step. For bromide potassium in water, the simulations have been done using 864 molecules in the liquid phase at different molalities and at the temperature of 298 K and 1 bar of pressure. The molality concentration is obtained from the total number of ions in solution  $N_{ions}$ , the number of water molecules  $N_{H_2O}$  and the molar mass of water  $M_{H_2O}$  as:

$$[KBr] = \frac{N_{ions} \times 10^3}{2N_{H_2O}M_{H_2O}}. \quad (3)$$

The division by 2 in this equation accounts for a pair of ions and  $M_{H_2O} = 18 \text{ g mol}^{-1}$ . The Table 3 gives the value of the molality for each point of calculus

The static dielectric constant is computed from the fluctuations [25] of the total dipole moment  $\mathbf{M}$ ,

$$\epsilon = 1 + \frac{4\pi}{3k_B T V} (\langle \mathbf{M}^2 \rangle - \langle \mathbf{M} \rangle^2) \quad (4)$$

where  $k_B$  is the Boltzmann constant and  $T$  the absolute temperature. The dielectric constant is obtained for long simulations at constant density and temperature or at constant temperature and pressure. The shear viscosity is obtained using the autocorrelation function of the off-diagonal components of the pressure tensor  $P_{\alpha\beta}$  according to the Green–Kubo formulation,

$$\eta = \frac{V}{k_B T} \int_0^\infty \langle P_{\alpha\beta}(t_0)P_{\alpha\beta}(t_0 + t) \rangle_{t_0} dt, \quad (5)$$

**Table 4**

Density of KBr at 1 bar of pressure and 298 K of temperature, Lattice Energy, Lattice Crystal of various Force Fields and for experiments [19].

Model ions	$\rho$ /(g/cm <sup>3</sup> )	LC/Å	LE/(kJ/mol)
JC <sub>S3</sub> [26]	2.61	6.66	695.38
JC <sub>T4</sub> [7]	2.67	6.62	698.72
KBr/ $\epsilon$	2.76	6.58	582.9
Experimental [19]	2.74	6.6	671.11

**Table 5**

ion–water Coordination Numbers obtained by our simulations along the r-range used in the integration.

Molal Concentration	MD KO	MD BrO
3.07	5.38	5.13
5	4.71	4.51

**Table 6**

Force field parameter of KCl/ $\epsilon$ .

Model	$q/e$	$\lambda_c$	$\sigma/\text{Å}$	$(\epsilon/k_B)/K$
K	+1	0.885	2.86	115.83
Cl	−1	0.885	3.85	192.45

## 4. Results

### 4.1. The KBr/ $\epsilon$ model

The parameters for KBr/ $\epsilon$  model were selected to reproduce the density of the crystal at the 298 K and 1 bar, namely 2.74 g cm<sup>−3</sup> [19] and the to show the peak in the radial distribution at 3.29 Å in agreement with the experiments [19]. The final step of the model is obtained by adjusting the parameters to give the correct dielectric constant of the 4 molal solution of the salt in water.

The Table 4 shows a comparison of the values obtained for the density, the Lattice Energy and the Lattice Crystal for the KBr/ $\epsilon$  model, for the experiments [19], for the Joung–Cheatham [7], the JC force field, and for the force field parametrized with SPC/E water, the JC<sub>S3</sub> model [26]. Our model gives good agreement with the experiments [19] in the density of the crystal and the Lattice Constant, but is 13% far from the reproduction of the Lattice Energy what indicates that our approximation understructure the salt what is a reflection of the parametrization in the water solution where the model is designed to primary employed.

In order to test the validity of our approach a number of thermodynamic and dynamic properties were computed for a variety of densities in addition to the density for which it was parametrized. The Fig. 2 illustrates the dielectric constant, the density and the viscosity versus molal concentration for the KBr/ $\epsilon$  model with the TIP4P/ $\epsilon$  water. The obtained with our model were compared with the experiments [19] and with other theoretical approaches such as the JC<sub>S3</sub> [26] and the JC<sub>T4</sub> [7] models. The dielectric constant and the molal concentration employed to parametrize the KBr/ $\epsilon$  is shown with a purple circle in Fig. 2(a). The result shows that our model gives a good agreement with the experiments when compared with the other theories. Comparison with other similar parametrizations using the dielectric constant screening were not possible since these thermodynamic and dynamic quantities were not computed for these approaches [13].

The water coordination numbers around the K and Br ions, shown in Table 5, was estimated by integrating the area under the first peak of the K–O and Br–O radial distribution functions shown in Fig. 3 up to the first minimum respectively.

### 4.2. The KCl/ $\epsilon$ model

One major drawback of our model is that in principle for each salt a new parametrization should be required. In order to avoid this limitation, we assume that since our parametrization relies in the hydration of water, any monovalent cation (anion) will have the same parameter when making a salt with other monovalent anion (cation). Then the KCl model does not require any further parametrization. Since both NaCl/ $\epsilon$  and KBr/ $\epsilon$  models have been already parametrized, we test the transferability of these two force fields as follows. Instead of fitting the parameters for the KCl from experiments, the parameters for the K are taken from the KBr/ $\epsilon$  given in the Table 1 while the parameters for the Cl are taken from the NaCl/ $\epsilon$  model [11]. The parameters for the KCl are summarized in Table 6. It is important to notice that no additional parametrization was needed for obtaining the KCl/ $\epsilon$  model.

In order to test if our assumption of the transferability of the ionic parametrization thermodynamic and dynamic properties were computed for the model and compared with the experiments and other models. First, the density of the

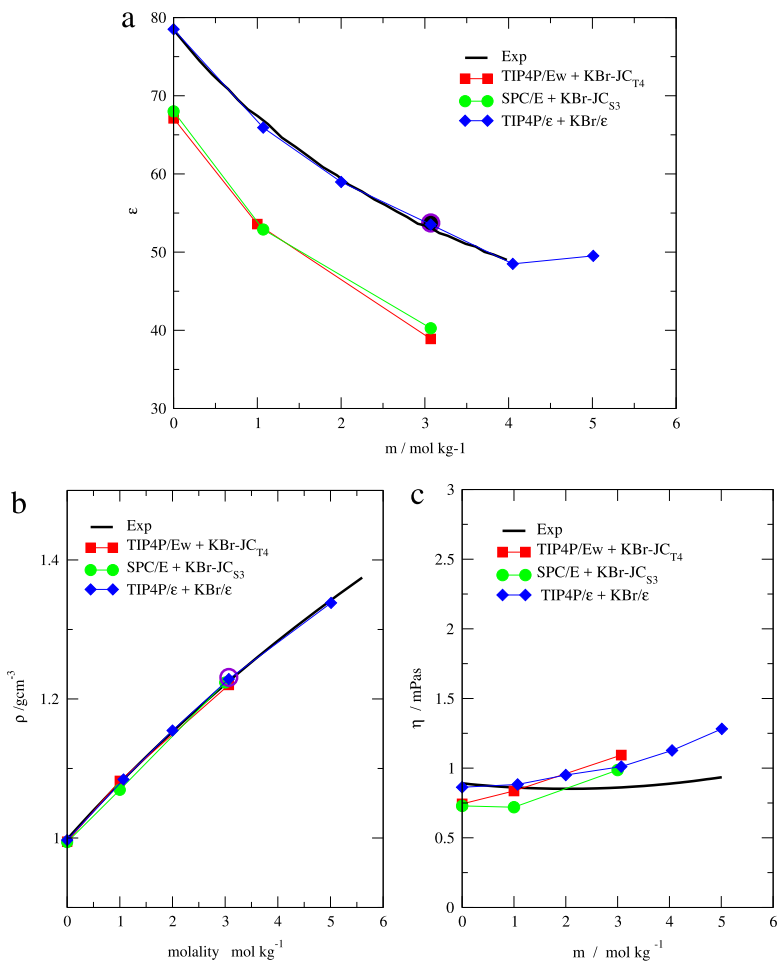


**Fig. 2.** (a) Dielectric constant, (b) density and (c) viscosity versus molal concentration of the KBr salt at 1 bar and 298 K. The black line is the experimental data [19], the blue filled diamond is the results for the KBr/ε model, the green spheres are the results for the JC<sub>S3</sub> model while the red squares are the results for the JC<sub>T4</sub> model. The violet circle in the figure (a) shows the concentration used for the parametrization of the model.

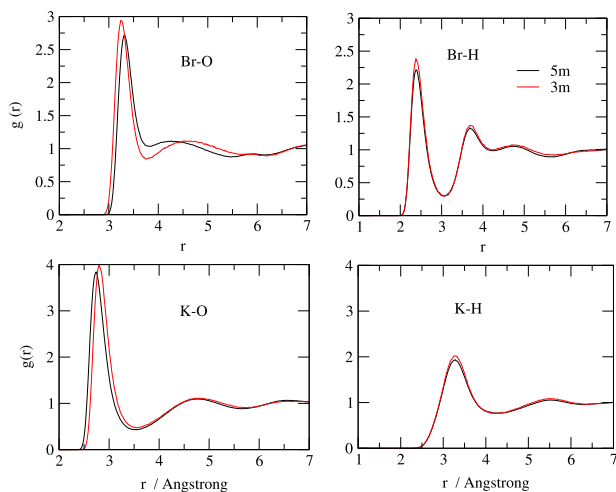


**Fig. 3.** ion–water pair distribution functions using the rigid water model TIP4P/ε and KBr/ε force field at 298 K, 1 bar, and ionic concentrations of 5 (black line) and 3 (red line) molal. In all cases 864 molecules were used. (For interpretation of the references to colour in this figure legend, the reader is referred to the web version of this article.)

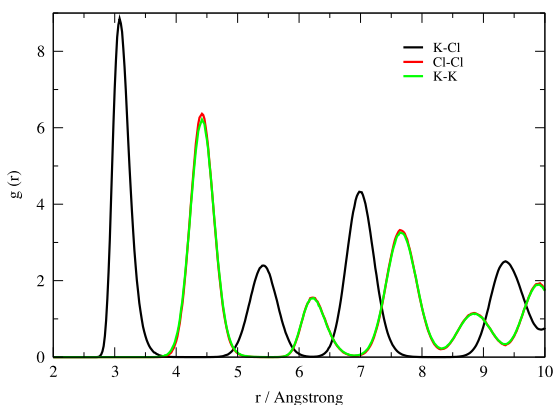


**Fig. 4.** Radial distribution function  $g(r)$  versus the distance  $r$  at 1 bar and 298 K for: Cl–Cl (red line), K–K (green line), and K–Cl (black line). (For interpretation of the references to colour in this figure legend, the reader is referred to the web version of this article.)

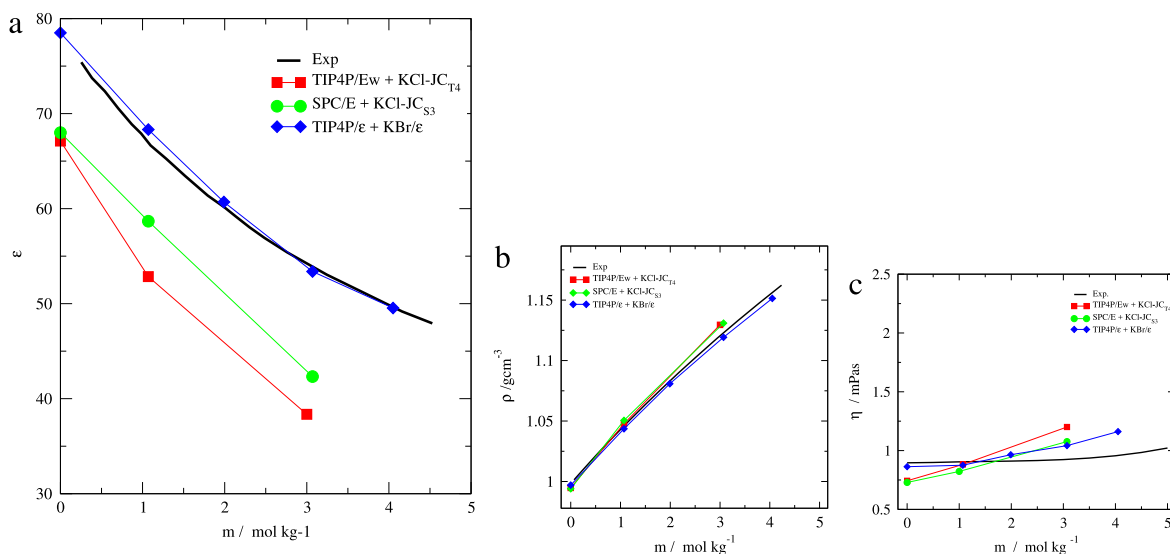


**Fig. 5.** (a) Dielectric constant, (b) density and (c) viscosity versus molal concentration of the salt at 298 K and 1 bar. The black line is the experimental data [19] and the blue filled diamond is the results of our model. All data are at room conditions.

**Table 7**

Density of KCl at 1 bar of pressure and 298 K of temperature, Lattice Energy, Lattice Crystal of various force fields and for experiments [19].

Model ions	$\rho / (\text{g}/\text{cm}^3)$	LC/Å	LE/(kJ/mol)
JC <sub>S3</sub> [26]	1.86	6.38	720.9
JC <sub>T4</sub> [7]	1.90	6.34	724.6
KBr/ $\epsilon$	1.99	6.29	600.77
Experimental [19]	1.99	6.26	720.06

crystal of KCl/ $\epsilon$  at the 298 K and 1 bar of pressure was computed. Our result gives  $1.99 \text{ g cm}^{-3}$  which is the same as the experimental data [19]. The radial distribution for K–K, Cl–Cl and K–Cl is illustrated in Fig. 4 and it shows a peak at  $3.08 \text{ \AA}$  in agreement with the experiments [19].

Nexr, the Lattice Constant (LC) at 1 bar of pressure and 298 K of temperature, illustrated in Table 7, was also calculated and it is in accordance with the experimental values [19]. The Lattice Energy (LE), however, it is 16.5% far from the reproduction of the Lattice Energy. This difference was present in the NaCl/ $\epsilon$  and KBr/ $\epsilon$  and models.

Finally, the (a) dielectric constant, (b) the density and the (c) the viscosity of the solution as a function of the molal concentrations is shown in Fig. 5 giving a good agreement with the experiments [19].

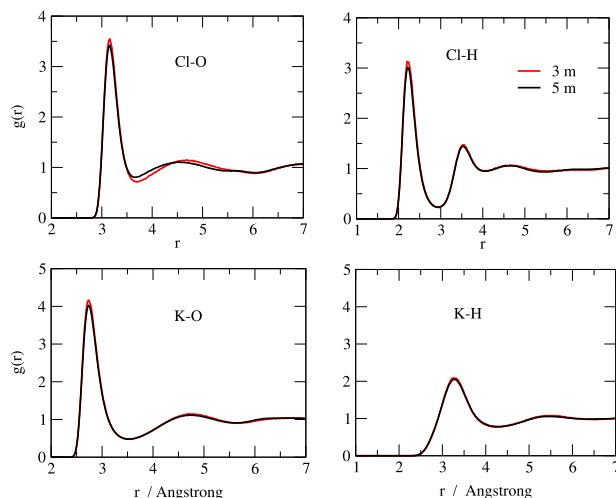


**Fig. 6.** ion–water pair distribution functions using the rigid water model TIP4P/ε and KCl/ε force field at 298 K, 1 bar, and ionic concentrations of 5 (black line) and 3 (red line) molal. In all cases 864 molecules were used. (For interpretation of the references to colour in this figure legend, the reader is referred to the web version of this article.)

**Table 8**

ion–water Coordination Numbers obtained by our simulations and experiments. The uncertainties of experimental data [27] are reported within parenthesis, along with the r–range used in the integration.

Molal Concentration	MD KO	MD ClO	Exp [28] KO
3.07	5.61	5.46	5.7
5	5.18	5.10	5.1

**Table 9**

Force field parameter of NaBr/ε.

Model	q/e	λ <sub>c</sub>	σ/Å	(ε/k <sub>B</sub> )/K
Na	+1	0.885	2.52	17.44
Br	−1	0.885	4.057	287.47

**Table 10**

Density of NaBr at 1 bar of pressure and 298 K of temperature, Lattice Energy, Lattice Crystal of various force fields and for experiments [19].

Model ions	ρ/(g/cm <sup>3</sup> )	LC/Å	LE/(kJ/mol)
JC <sub>s3</sub> [26]	3.00	6.06	761.48
JC <sub>r4</sub> [7]	3.09	6.00	766.50
NaBr/ε	3.2	5.90	600.77
Experimental [19]	3.2	5.97	753.95

Using the radial distribution functions respect to oxygen of the cation and anion at different concentrations. We calculated the number of coordination around the K and Cl, we do this through the integration the area under the first peak of the K–O and Cl–O pair distribution functions up to the first minimum respectively of the Fig. 6. These coordination numbers are shown in Table 8 and give a good agreement with the experiments in the case of KO.

#### The NaBr/ε model

The consistency of the new force fields was also checked by creating the NaBr/ε model employing the parameters for Br and Na, shown in Table 9, extracted from the force fields for the KBr/ε and NaCl/ε models respectively. The radial distribution for Na–Na, Br–Br and Na–Br are illustrated in Fig. 7. The density of the crystal, the lattice energy and the lattice constant are shown in Table 10 showing a good agreement with the experimental results.

The Fig. 8 illustrates the dielectric constant, the density and the viscosity versus molal concentration of the NaBr/ε salt model in solution with the TIP4P/ε water. The graphs show that the new model gives a better agreement with the experiments than the other atomistic parameterizations.

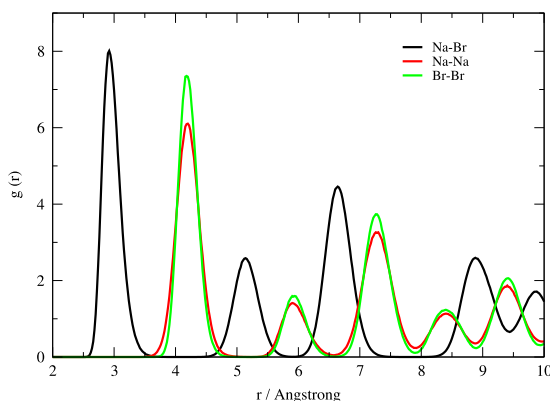


**Fig. 7.** Radial distribution function  $g(r)$  versus the distance  $r$  at 1 bar and 298 K for: Na–Na (red line), Br–Br (green line), and Na–Br (black line). (For interpretation of the references to colour in this figure legend, the reader is referred to the web version of this article.)

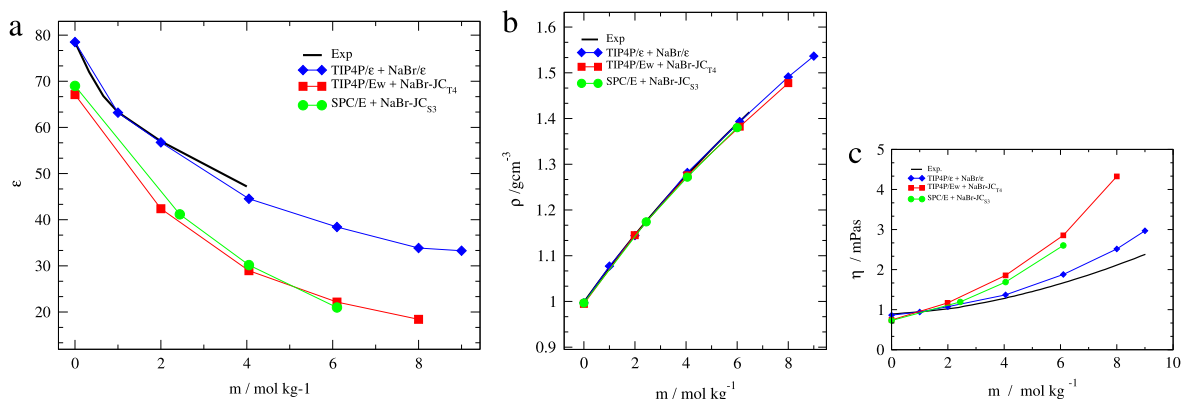


**Fig. 8.** (a) Dielectric constant, (b) density and (c) viscosity versus molal concentration of the salt. The black line is the experimental data [19] and the blue filled diamond is the results of our model. All data are at room conditions. Violet circle in the case (a) is for the diluted concentration where was made the parametrization.

**Table 11**  
ion–water Coordination Numbers obtained by our simulations.

Molal Concentration	MD NaO	MD BrO
4	4.62	13.8
6	4.14	14.11
9	3.65	12.86

The ion–water radial distribution functions are illustrated in Fig. 9. Employing this functions, the coordination around the NA and Br were computed and shown in Table 11.

The solubility of  $\text{KBr}/\varepsilon$ ,  $\text{KCl}/\varepsilon$  and  $\text{NaBr}/\varepsilon$  was calculated with the method proposed by Dominguez et al. [29] and we obtained values closed to the experimental data. In a future work we present this calculus.

## 5. Conclusions

In this paper a new force field for the  $\text{KBr}/\varepsilon$  was proposed. The model is parametrized under the assumption that the ions interactions are screened by the water and part of this effect is taken into account by a parametrized Coulombic force.

We show that our model reproduces the density of the crystal and structure, as well as the thermodynamic and dynamic properties of the solution with the TIP4P/ $\varepsilon$  model for water at different molal concentration. It particularly reproduces the dielectric constant of the solution for a wide range of salt concentrations what is a property not well represented by the other atomistic models.

In order to test the transferability of the  $\text{KBr}/\varepsilon$  and of the  $\text{NaCl}/\varepsilon$  ions parametrization, the same parameters for the isolated ions were employed in the construction of the  $\text{KCl}/\varepsilon$  and of the  $\text{NaBr}/\varepsilon$  models. In the construction of these two new



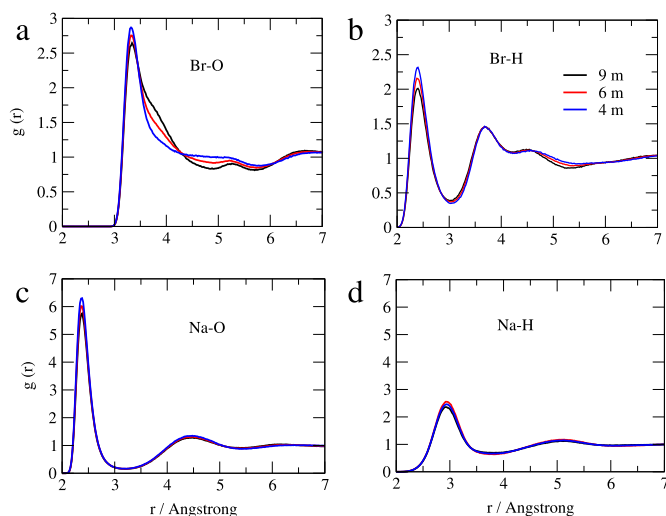


**Fig. 9.** The radial distribution function for (a) Br–O, (b) Br–H, (c) Na–O and (d) Na–H in TIP4P/ $\epsilon$  water with NaBr/ $\epsilon$  at salt concentrations of 9 (black line), 6 (red line) and 4 (blue line) molal. In all cases 864 molecules were employed. (For interpretation of the references to colour in this figure legend, the reader is referred to the web version of this article.)

models there was no an additional parametrization. The results of the density, the dielectric constant and the viscosity of the KCl/ $\epsilon$  and of the NaBr/ $\epsilon$  models reproduce well the experiments. Since our models give a very robust result for the dielectric constant, we believe that they are suitable for studying confined systems and can be used to study ionic channels.

## Acknowledgments

We thank the Brazilian agencies CNPq, INCT-FCx, and Capes for the financial support. We also thank the SECITI of Mexico city for financial support.

R.F.A. thanks José Alejandro Ramirez chief of the Chemistry Department at UAM-Iztapalapa in Mexico city for all the advice and helpful discussions.

## References

- [1] I.D. Weiner, S. Linus, C.S. Wingo, in: R. Johnson, J. Fluege, J. Feehally (Eds.), *Comprehensive Clinical Nephrology*, fourth ed., Saunders Elsevier, 2010, pp. 118–129.
- [2] G. Malnic, G. Giebisch, S. Muto, W. Wang, M.A. Bailey, L.M. Satlin, *Inphysiology and pathophysiology*, in: R.J. Alpern, M.J. Caplan, O.W. Moe (Eds.), *Seldin and Giebisch'S the Kidney*, fifth ed., Academic Press, London, 2013, pp. 1659–1716.
- [3] D.B. Mount, K. Zandi-Nejad, *Disorders of potassium balance*, in: Brenner & Rector's the Kidney, ninth ed., Elsevier, 2007, pp. 640–672.
- [4] A.S. McCall, C.F. Cummings, G. Bhave, R. Vanacore, *Cell* 157 (2014) 1380.
- [5] A.N. Mayeno, A.J. Curran, R.L. Roberts, C.S. Foote, *J. Biol. Chem.* 264 (1989) 5660.
- [6] M.P. Patricelli, J.E. Patterson, D.L. Boger, B.F. Cravatt, *Bioorg. Med. Chem. Lett.* 8 (1998) 613.
- [7] I.S. Joung, T.E. Cheatham III, *J. Phys. Chem. B.* 112 (2008) 9020.
- [8] E. Sanz, C. Vega, *J. Chem. Phys.* 126 (2007) 014507.
- [9] D. Corradini, M. Rovere, P. Gallo, *J. Chem. Phys.* 132 (2010) 134508.
- [10] Y. Liu, T. Lafitte, A.Z. Panagiotopoulos, P.G. Debenedetti, *AIChE J.* 59 (2013) 3514.
- [11] R. Fuentes-Azcatl, M.C. Barbosa, *J. Phys. Chem. B.* 120 (2016) 2460.
- [12] I.V. Leontyev, A.A. Stuchebrukhov, *J. Chem. Phys.* 141 (2014) 014103.
- [13] Z.R. Kann, J.L. Skinner, *J. Chem. Phys.* 141 (2014) 104507.
- [14] A.H. Mao, R.V. Pappu, *J. Chem. Phys.* 137 (2012) 064104.
- [15] R. Fuentes-Azcatl, J. Alejandro, *J. Phys. Chem. B.* 118 (2014) 1263.
- [16] R. Fuentes-Azcatl, M.C. Barbosa, *Physica A* 444 (2016) 86.
- [17] R. Fuentes-Azcatl, N. Mendoza, Alejandro, J., *Improved SP C force field of water based on the dielectric constant: SPC/ $\epsilon$* , *Physica A* 420 (2015) 116.
- [18] J.P. Hansen, I.R. McDonald, *Theory of Simple Liquids*, third ed., Academic, Amsterdam, 2006.
- [19] D.R. Lide, *CRC Handbook of Chemistry and Physics*, ninetyth ed., CRC Press, Cleveland, OH, USA, 2009.
- [20] M.J. Abraham, D. van der Spoel, E. Lindahl, B. Hess, GROMACS development team, *GROMACS User Manual version 5.0*, 2014. [www.gromacs.org](http://www.gromacs.org).
- [21] M.P. Allen, D.J. Tildesley, *Computer Simulation of Liquids*, Oxford University Press, Oxford, UK, 1987.
- [22] U. Essmann, L. Perera, M.L. Berkowitz, T. Darden, H. Lee, L.G. Pedersen, *J. Chem. Phys.* 103 (1995) 857.
- [23] B. Hess, H. Bekker, H.J.C. Berendsen, J.G.E.M. Fraaije, *J. Comput. Chem.* 18 (1997) 1463.
- [24] M.E. Tuckerman, Y. Liu, G. Ciccotti, G.J. Martyna, *J. Chem. Phys.* 115 (2001) 1678.
- [25] M. Neumann, *Mol. Phys.* 50 (1983) 841.
- [26] D.E. Smith, L.X. Dang, *J. Chem. Phys.* 100 (1994) 3757.
- [27] R. Mancinelli, A. Botti, F. Bruni, M.A. Ricci, A.K. Soper, *J. Phys. Chem. B* 111 (2007) 13570.

[28] M. Yizhak, *Chem. Rev.* 88 (1988) 1475.

[29] H. Manzanilla-Granados, H. Saint-Martin, R. Fuentes-Azcatl, J. Alejandro, *J. Phys. Chem. B.* 119 (2015) 8389.